RSC Advances

REVIEW

View Article Online
View Journal | View Issue

Check for updates

Cite this: *RSC Adv.*, 2023, **13**, 31687

Polymer-based nanocomposite adsorbents for resource recovery from wastewater

Aminat Mohammed Ahmed,[abc] Menbere Leul Mekonnen [ab] and Kebede Nigussie Mekonnen *[abd]

Developing mitigation mechanisms for eutrophication caused by the uncontrolled release of nutrients is in the interest of the scientific community. Adsorption, being operationally simple and economical with no significant secondary pollution, has proven to be a feasible technology for resource recovery. However, the utility of adsorption often lies in the availability of effective adsorbents. In this regard, polymer-based nanocomposite (PNC) adsorbents have been highly acclaimed by researchers because of their high surface area, multiple functional groups, biodegradability, and ease of large-scale production. This review paper elaborates on the functionality, adsorption mechanisms, and factors that affect the adsorption and adsorption–desorption cycles of PNC adsorbents toward nutrient resources. Moreover, this review gives insight into the application of recovered nutrient resources in soil amendment.

Received 11th August 2023
Accepted 16th October 2023

DOI: 10.1039/d3ra05453e

rsc.li/rsc-advances

Open Access Article. Published on 30 Thang Mi 2023. Downloaded on 01/06/2026 7:15:53 CH.
This article is licensed under a Creative Commons Attribution-NonCommercial 3.0 Unported Licence.

1. Introduction

1.1. Nutrient pollution and its effect on water

Resource recovery is the process of recovering materials or energy from waste for reuse.[1] In the 21st century, the development of industrialization, urbanization, and advancement of agricultural practices has caused an uncontrolled discharge of pollutants into the aquatic system. Excess nutrient inputs (phosphorous and nitrogen) to water bodies come from point and nonpoint sources, like industrial discharges, agricultural runoff (animal and crop farming), and urban sewage. These released nutrients affect water quality and aesthetics. On the other hand, nutrients are finite resources that require recycling from various sources. The deterioration of water quality is caused by the overgrowth of phytoplankton and invasive weeds in aquatic environments, which results in the escalation of eutrophication.[2] Thus, eutrophication heightens the consumption of dissolved oxygen (DO) in the water, resulting in the depletion of DO in the aquatic environment. The depletion of DO leads to increases in both chemical oxygen demand (COD) and biological oxygen demand (BOD). Indeed, water quality deterioration leads to the loss of aquatic communities and a decrease in the aesthetic value of water.[3] Thus, recovering

[a]*Department of Industrial Chemistry, College of Natural and Applied Sciences, Addis Ababa Science and Technology University, P.O. Box 16417, Addis Ababa, Ethiopia. E-mail: kebede.nigussie@aastu.edu.et*

[b]*Nanotechnology Centre of Excellence, Addis Ababa Science and Technology University, P.O. Box 16417, Addis Ababa, Ethiopia*

[c]*Department of Chemistry, College of Natural Sciences, Wollo University, P.O. Box 1145, Dessie, Ethiopia*

[d]*Department of Chemistry, College of Natural and Computational Sciences, Mekelle University, P.O. Box 231, Mekelle, Ethiopia*

Aminat Mohammed Ahmed

Mrs. Aminat Mohammed Ahmed received her MSc in Analytical Chemistry from Dilla University, Ethiopia. Her research focuses on polymer based nanocomposite adsorbents for nutrient recovery. Mrs Aminat is currently a PhD student of Analytical Chemistry at Addis Ababa Science and Technology University in Ethiopia.

Menbere Leul Mekonnen

Menbere Leul Mekonnen received his PhD in Applied Analytical Chemistry from the National Taiwan University of Science and Technology in Hwang's group. His research focuses on nanoplasmonics, surface-enhanced Raman spectroscopy (SERS), sensors, and nanosorbents for nutrient recovery. Dr Menbere is currently an Assistant Professor of Analytical Chemistry at Addis Ababa Science and Technology University in Ethiopia.

© 2023 The Author(s). Published by the Royal Society of Chemistry

Open Access Article. Published on 30 Thang Mi 2023. Downloaded on 01/06/2026 7:15:53 CH.
This article is licensed under a Creative Commons Attribution-NonCommercial 3.0 Unported Licence.

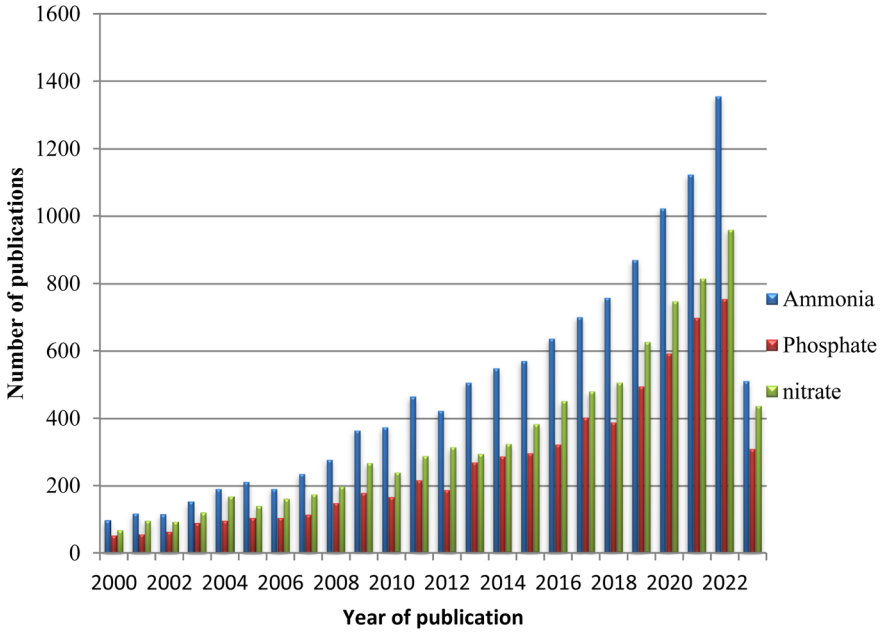

Fig. 1 Number of publications per year on nutrient removal from 2000–2023 (source Scopus database, accessed on May 04, 2023).

nutrients from wastewater is highly demanded for the sustainable use of natural resources.[1]

The effect of nutrients as a cause of eutrophication has been reported in different parts of the world. For example, the concentration of NO_3^- (59.5–84.5 mg L^{-1}) in Lake Idku located in Egypt was reported as a cause of chlorophyll *a* (Chl-*a*) concentration (0.051–0.102 mg Chl-*a* L^{-1}) and total phytoplankton cell count (269–1425 unit per mL) in different species of algae.[4] In another study, the PO_4^{3-} and NO_3^- concentrations of 0.020–0.100 mg L^{-1} and 0.26–3.60 mg L^{-1}, respectively, in three rivers of Cotê d'Ivoire caused Chl-*a* concentrations of 0.062–0.164 mg L^{-1}.[5] In the case of Ethiopia, the NO_3^- (0.28–1.56 mg L^{-1}) and PO_4^{3-} (0.51–1.77 mg L^{-1}) concentrations caused a mean concentration of Chl-*a* of 0.027–0.050 mg L^{-1}.[6] The maximum EPA limit for phosphorous in effluent is 1 mg L^{-1}, while it is 3 mg L^{-1} for total nitrogen.[7,8] Indeed, eutrophication leads to diversity loss and decreases the aesthetic value of aquatic systems.[9,10] To overcome such environmental problems, nutrient/resource recovery has been proposed as a mitigation mechanism. Herein, the techniques and various factors affecting the advancement of adsorptive resource recovery from wastewater are reviewed.

Kebede Nigussie Mekonnen

Kebede Nigussie Mekonnen received his PhD in Analytical Chemistry from Addis Ababa University in Ethiopia. He is working on nanomaterials for the detection of target analytes/pollutants and nutrient recovery and the analysis of elemental pollutants and persistent organic pollutants (POPs) in aquatic environment, soil/sediment, and/or biota. His research interests are the analysis of potentially toxic elements and organic pollutants in various matrices; recycling of wastes and usage of pretreated wastes for other activities; and nanomaterials for detection of analytes. Dr Kebede is currently an Associate Professor of Analytical Chemistry at Addis Ababa Science and Technology University in Ethiopia.

1.2. Existing methods of nutrient removal and recovery from wastewater

The eutrophication caused by the excessive release of nutrients brings algal bloom and decreases the water quality. Due to this, the development of mechanisms for removal and recovery has received great attention from researchers for the last two decades. The number of publications on the development of phosphate, nitrate, and ammonia removal and recovery methods dramatically increased (Fig. 1). From the graph, it can be seen that from 2000–2010, the number of publications is small, indicating that the pollution level and the concern were less. However, in recent times, the removal and recovery of nutrients from polluted water has become a serious concern to the world. This indicates that the world community is highly concerned with mitigation mechanisms for eutrophication. Consequently, different methods have been explored for the purification of wastewater and recovering contaminants as a resource.

For the past few decades, various physicochemical and biological methods have been developed for the removal and recovery of nutrients from wastewater. Among the common methods for the removal and recovery of resources, biological

© 2023 The Author(s). Published by the Royal Society of Chemistry

Open Access Article. Published on 30 Thang Mi 2023. Downloaded on 01/06/2026 7:15:53 CH. This article is licensed under a Creative Commons Attribution-NonCommercial 3.0 Unported Licence.

Table 1 Advantages and limitations of different techniques employed in nutrient resource removal

No.	Removal techniques	Advantages	Limitations	References
1	Membrane filtration	High surface area, uniformity of pore-size, and better removal efficiency	Membrane fouling, membrane deposition, process complexity, and low permeate current	22 and 27
2	Ion exchange	Good removal efficiency	Resin fouling, regeneration difficulty, reversible side reaction	23 and 28
3	Coagulation and flocculation	Can be done at any temperature	High coagulant requirement, high sludge production, and low efficiency	24
4	Chemical precipitation	Good removal efficiency	Secondary pollution, sludge formation, and inhibitory effects on the biological process	29
5	Biological treatment	Low cost	Time-intensive, incomplete removal	23
6	Ozonization	Good removal efficiency	Secondary pollution due to oxidation	25
7	Electrochemical methods	Good removal efficiency	Secondary pollution, high cost	26 and 30
8	Anaerobic (ammonia) oxidation	No need of oxygen reduced sludge	Incomplete nitrogen removal	31

treatment,[11,12] membrane filtration,[13,14] precipitation and coagulation,[15,16] ion exchange,[17,18] and adsorption[14] techniques have been employed. Moreover, methods like anaerobic ammonium oxidation[19] and ozonization[20] for ammonia–nitrogen removal and electrochemical methods[21] have been used in the removal and recovery of nutrient resources.

The above mentioned methods have been recognized as good techniques regarding removal efficiency. However, there are some limitations associated with these methods (Table 1). For example, the membrane filtration method has good removal efficiency due to its features like uniform pore-size distribution. However, membrane fouling, membrane deposition, and process complexity have been considered shortcomings of the method.[22] The biological method is eco-friendly, with drawbacks like time consumption and incomplete elimination in some cases.[23] Chemical precipitation and photodegradation are better techniques for the reduction of pollutants. However, these methods suffer from secondary pollution.[24,25] The electrochemical and ion exchange methods are high-cost and considered less efficient.[26] Consequently, adsorption is considered an alternative method in the removal and recovery of nutrients from wastewater. The adsorption process participates in the recovery of nutrients using environmentally benign adsorbent materials, so that the recovered nutrients can be reused.

1.3. Advancement in adsorption for nutrient recovery

In the past few years, the recovery of nutrients from wastewater has become advanced. Unlike other methods, resource recovery through adsorption by surface-enhanced materials offers a simple and economically beneficial method which follows a simple adsorption/desorption process employed in the decrement of nutrient content in different water streams. In this context, adsorption by functionalized graphene oxide,[32] nanobiochar,[33–35] metal-doped activated carbon,[36,37] metal oxide/hydroxide nanoparticle,[38,39] metal–organic framework (MOF),[40] surface-enhanced zeolite,[41] and polymer-based nanocomposite (PNC) adsorbents[42] has shown better removal and recovery performances of nutrient resources from wastewater. Indeed, the efficiency of adsorbents can be significantly improved through surface modification.[43,44] Table 2 shows some common types of surface-enhanced adsorbents and their adsorption mechanisms toward nutrients from wastewater. Thus, the mechanisms of pore filling through the physisorption process, electrostatic interaction of ions with surfaces, precipitation on the metallic surface, ligand exchange, and complexation are common trapping methods in adsorption.[33,45]

Enhanced adsorption efficiency of adsorbent materials can be achieved through different modification mechanisms. For example, thermally treated activated carbon (AC) removed 0.82 mg g^{-1} PO_4^{3-}.[46] However, sludge-based activated carbon functionalized with MgAl double-layered hydroxide (SBAC-MgFe) composites removed 110 and 54.5 mg g^{-1} of PO_4^{3-} and NO_3^-, respectively.[37] A strontium-modified magnetic graphene oxide (MGO-Sr) nanocomposite removed 238.09 and 357.14 mg g^{-1} of PO_4^{3-} and NO_3^-, respectively. The MGO-Sr follows a physisorption mechanism with a monolayer formation process, and the electrostatic attraction of PO_4^{3-} and NO_3^- for Sr^{2+} removed 91 and 80% PO_4^{3-} and NO_3^-, respectively, in the presence of coexisting ions (Table 2).[47] Though the better efficiency of carbon-based materials is exhibited by their porosity and high surface area, the adsorption process can be affected by co-existing ions.[48] Similarly, zeolites are not very effective in nutrient adsorption without modification. Modification with

Open Access Article. Published on 30 Thang Mi 2023. Downloaded on 01/06/2026 7:15:53 CH.
This article is licensed under a Creative Commons Attribution-NonCommercial 3.0 Unported Licence.

Table 2 Some common types of surface-enhanced adsorbents for the removal of PO_4^{3-}, NO_3^-, and NH_4^+

No.	Adsorbent	Synthesis method	Adsorbate	Adsorption capacity (mg g^{-1})	Kinetics/isotherm	Interference	Other optimal factors	References
1	Zirconium-loaded reduced graphene oxide	Hydrothermal method	PO_4^{3-}	27.71	Pseudo-second-order/ Langmuir isotherm model	SO_4^{2-}, F^-, Cl^-, NO_3^-, and CO_3^{2-}	pH = 5, T = 298 K	32
2	Lanthanum oxide supported on activated carbon	Chemical impregnation	PO_4^{3-}	21.14	Pseudo-second-order/ Langmuir isotherm	—	T = 310–323 K, pH = 7	53
3	Fe/Zr modified activated carbon nanofiber	Coprecipitation method	PO_4^{3-}	26.3	Pseudo-second-order/ Langmuir model	F^-, NO_3^-, Cl^-, and SO_4^{2-}	pH = 4	54
4	CaO–biochar composites	Ball milling and pyrolysis	PO_4^{3-}	231	Pseudo-second-order/ Langmuir model	—	pH = 5–11, T = 318	34
5	Lanthanum-modified platanus biochar	Coprecipitation method	PO_4^{3-}	148.11	Pseudo-second order/ Langmuir model	SO_4^{2-}, NO_3^-, HCO_3^-, CO_3^{2-}, and Cl^-	pH = 3–9	45
6	Strontium magnetic graphene oxide nanocomposite	Modified hummers method	NO_3^- and PO_4^{3-}	357.14 and 238.09	Pseudo-second-order/ Langmuir isotherm	SO_4^{2-}, Br^-, Na^+, K^+, Zn^{2+}, Cu^{2+}, Fe^{3+}, and Cl^-	pH = 5–8, adsorbent dose = 30 mg, time = 90 min	47
7	Magnetic Mg–Fe/LDH activated carbon composites	Coprecipitation method	NO_3^- and PO_4^{3-}	54.5 and 110	Pseudo-first-order/ Langmuir and Freundlich models	Cl^-, CO_3^{2-}, and SO_4^{2-}	pH = 3, adsorbent dose = 5 mg, contact time = 250 min, and T = 298 K	37
8	La-MOFs	Solvothermal method	PO_4^{3-}	142.04	Pseudo-second-order/ Langmuir isotherm model	—	pH = 4–8, adsorbent dosage = 0.02 g, time = 20 min	55
9	Al-BC and Mg-BC	Pyrolysis	PO_4^{3-}	44.8 and 56.1	Pseudo-first-order/ Langmuir model	—	pH = 6, adsorbent dosages = 0.1 g	35
10	Mg/Zr modified nanobiochar	Hydrothermal method	PO_4^{3-}	39.4	Pseudo-second-order model/Freundlich isotherm	Cl^-, NO_3^-, CO_3^{2-} and SO_4^{2-}	pH = 1, adsorbent dose = 40 mg, contact time = 70 min	33
11	Organic modified Al/Mn bimetal oxide	Coprecipitation method	NO_3^- and PO_4^{3-}	19.45 and 33.16	Pseudo-second order and Elovich model/ Langmuir model	—	pH = 4, T = 298 K	38
12	*Eupatorium adenophorum* biochar	Pyrolysis	PO_4^{3-} and NH_4^+	2.32 and 1.909	Pseudo-second-order/ Langmuir-Freundlich model	Na^+, K^+, Ca^{2+}, Fe^{3+}, Cl^-, CO_3^{2-}, SO_4^{2-}, NO_3^-	pH = 8.0, adsorbent dose = 0.5 g	56
13	La-MOFs	Solvothermal method	NO_3^- and PO_4^{3-}	49.73 and 62.80	Pseudo-second order and intraparticle diffusion model/ Freundlich isotherm	SO_4^{2-}, $HCrO_4^-$, HCO_3^-, Cl^- and F^-	pH = 5 for NO_3^-, pH = 7 for PO_4^{3-}, adsorbent dosage = 0.1 g, time = 30 min	40
14	Mg/Al-modified biochar	Pyrolysis	NO_3^-, PO_4^{3-} and NH_4^+	40.63, 74.47, and 0.7, respectively	Pseudo-first-order and pseudo-second-order models	—	pH = 7.9	57
15	Mg/Al layered double hydroxide modified biochar	Pyrolysis	NO_3^-	156.84	Pseudo-second-order/ Freundlich model	NH_4^+	pH = 3–9, adsorbent dosage = 0.1 g	58
16	FeAC@Sr	Coprecipitation method	NO_3^-	87.42	Pseudo-second-order/ Langmuir isotherm	—	pH = 4, adsorbent dosage = 60 mg	59

© 2023 The Author(s). Published by the Royal Society of Chemistry

Open Access Article. Published on 30 Thang Mi 2023. Downloaded on 01/06/2026 7:15:53 CH.
This article is licensed under a Creative Commons Attribution-NonCommercial 3.0 Unported Licence.

metal and metal oxide nanoparticles improves their adsorption efficiency *via* ion exchange, electrostatic interaction, hydrogen bonds, and inner sphere surface complexes. Accordingly, 84% of PO_4^{3-} was removed using a TiO_2-bentonite composite.[49] Thus, pristine zeolite has low adsorption efficiency, while the modified one showed better efficiency. This performance variation could be due to the replacement of zeolitic monovalent ions like Na^+ with interacting divalent metal cations like Ca^{2+} and Mg^{2+} ions.[50] Further, metal-based nanoparticles have excellent trapping ability towards PO_4^{3-} through adsorption. For example, the hydrothermally synthesized Ca–La layered double hydroxide (Ca–La LDH) removed 194.04 mg g^{-1} of PO_4^{3-} within 30 min. The physisorption and ion exchange mechanisms contributed the high adsorption capacity of Ca–La LDH and better selectivity towards PO_4^{3-}.[51] Moreover, MOF materials achieve better removal efficiency of nutrients. For example, a high surface area (1686 m^2 g^{-1}) iron-based MOF (Fe-MOF-808) removed 305.5 mg g^{-1} of PO_4^{3-} by physisorption and chemisorption mechanisms.[52] So far, different types of adsorbent materials have been blended with polymers to obtain better features in the adsorption of water contaminants, particularly nutrients.

2. Polymer-based nanocomposite materials for resource recovery from wastewater

Nanostructured polymeric composites are formed in the interface of nanoparticles and polymers.[60] PNC materials have received great attention because of their unique physicochemical properties like their availability, biodegradability, renewability, ease of synthesis, and multiple active reaction sites. Thus, the unique properties of PNCs make them important materials for the sorption of water contaminants.[61]

2.1. Overview of polymer-based nanocomposite adsorbents and their application in resource recovery

Adsorbents engineered from polymers have been used in the recovery of different types of contaminants found in wastewater. Polymer materials have attractive features, like high adsorption capacity, large surface area, ease of large-scale fabrication, active functional groups, and ease of functionalization, which qualify them as effective adsorbents.[62] However, polymer materials, particularly biopolymers,[63] have some limitations, like swelling and poor mechanical strength and stability.[64,65] In this regard, the chitosan extracted from fish, crab, and shrimp exhibited 492%, 138%, and 358% water binding capacity, respectively.[66] In another study, the water binding capacity of chitosan extracted from shrimp using different solvents was also reported as 554–638%.[67] A material having high swelling properties can lose its stability in water and be unfavourable for adsorption.

The mechanical strength and stability of some polymers are weak. For example, alginate has been reported to have low mechanical strength, and thus the addition of attapulgite exhibited a remarkable change in its mechanical strength.[68] Additionally, the modification of lignin with polyethyleneimine enhanced its stability in the adsorption/desorption cycle.[69] The incorporation of polyethyene polyamine into a chitosan–zirconium composite allowed it to undergo ten adsorption/desorption cycles and retain 73% of its initial adsorption capacity.[70] Thus, to overcome their limitations and improve their adsorption capacity, polymers have been modified with materials prepared from carbonaceous and noncarbonaceous substances to fabricate PNC adsorbents. As a result, the surface morphology and roughness of the PNC is enhanced, which could assist in rapid interfacial interactions.[71] In addition, incorporating nanomaterials into a polymer matrix could result in a material with good tensile strength and better surface functionality.[61,65] Thus, PNC materials are known for their versatile applications and their sustainability for the proper mitigation of environmental pollution-related issues.[72]

Polymer-based nanocomposite materials have shown enhanced adsorption capacity and tunability which are suitable for practical adsorptive resource recovery applications. From this perspective, polymers combined with activated carbon,[73] graphene oxide,[74] MOF,[75] metal/metal oxide,[1,76] zeolite,[77] and carbon nanotubes[78] have been employed in the removal and recovery of nutrient resources. Polymer-based hybrid materials exhibited a large surface area with a porous framework and multiple surface functionalities with better stability, making them attractive materials for adsorption applications.[65,79] Overall, the PNC facilitated the adsorption process through physisorption (physical transfer) and chemisorption (electrostatic interaction, ion exchange, hydrogen bonding, complexation, precipitation, *etc.*) mechanisms, as summarized in Table 3.

2.2. Functionality and efficiency of polymer-based nanocomposite adsorbents in the recovery of resources from wastewater

During the synthesis of PNC materials, new physicochemical properties can be exhibited which make the material interactive with another component for good mechanical strength and performance. Such characteristics are helpful for multiple applications, including the adsorption of nutrient resources. Thus, the surface area, porosity, and multiple functional groups of PNC make them attractive materials and are preferably applied in resource recovery.[72] Furthermore, the pH of a solution in which its variation affects the ionization degree of an adsorptive molecule and surface charge can influence the adsorption capacity of a PNC.[74] Further, the amount of adsorbent added is an important factor that affects the adsorbent capacity of adsorbents. Additionally, interfering ions that exist in a solution, contact time, and temperature are undeniable factors during experiments.[65,89]

2.2.1. Recovery of phosphate from wastewater by polymer-based nanocomposite adsorbents. Phosphorus is an important nutrient resource for plant growth; however, it causes eutrophication in water bodies.[90] The recovery of PO_4^{3-} from wastewater is of great concern for controlling eutrophication and in the sustainable use of phosphorus. PNC adsorbents are

Open Access Article. Published on 30 Thang Mi 2023. Downloaded on 01/06/2026 7:15:53 CH.
This article is licensed under a Creative Commons Attribution-NonCommercial 3.0 Unported Licence.

Table 3 Recovery of resources with different polymer-based nanocomposite adsorbents

No.	Polymer material	Nutrient	Adsorption capacity	Studied conditions	Surface area ($m^2\ g^{-1}$)	Resource concentration ($mg\ L^{-1}$)	Adsorption mechanism	References
1	$Mg_6Al_2(CO_3)(OH)_{16}4H_2O$ LDH chitosan nanocomposite	PO_4^{3-}	106.3 mg	pH and adsorbent doses	28.47	—	Electrostatic attraction	80
2	La/Fe–Cs composites	PO_4^{3-}	67.52 mg g^{-1}	pH, contact time, and co-existing ions	109.84	109.84	Precipitation, electrostatic attraction, and complexation	1
3	AL-PEI-La	PO_4^{3-}	65.79 mg g^{-1}	pH, temperature, and co-existing ions	85.78	—	Electrostatic attraction and ligand exchange	81
4	MFLC	PO_4^{3-}	906.82 mg g^{-1}	pH, temperature, and coexisting anions	140.81	100–1200	Single-layer chemisorption and ligand exchange	82
5	HPEI-EC	PO_4^{3-}	15.53 mg g^{-1}	pH, time, and coexisting anions	2.65	1.25	Electrostatic attraction	83
6	MPANI@La	PO_4^{3-}	45.24 mg g^{-1}	pH, time, initial concentration, temperature, and adsorbent dose	—	5–40	Ion exchange, electrostatic attraction, and Lewis acid–base interaction	42
7	Lignin-PEI-M	PO_4^{3-}	43 mg g^{-1}	pH, time, coexisting ions, and temperature	—	—	Ligand exchange, electrostatic attraction, and Lewis acid–base interaction	84
8	$Fe_3O_4$50%-PANI@GO	PO_4^{3-}	135.67 mg g^{-1}	pH, contact time, adsorbent dosage, initial concentration, and co-existing ions	57.99	100	Surface complexation and electrostatic attraction	85
9	Zr@AlgKN composite	NO_3^- and PO_4^{3-}	31.24 and 37.18 mg g^{-1}	pH, co-existing ions, contact time, and adsorbent doses	78.93	20–140	Electrostatic attraction, ion exchange, and complexation	86
10	TATGO@CS hybrid	NO_3^- and PO_4^3	58.46 and 61.38 mg g^{-1}	pH, time, sorbent dosage, and interfering ions	68.94	20–140	Electrostatic attraction	74
11	TATGO@Alg	NO_3^- and PO_4^{3-}	51.83 and 58.46 mg g^{-1}	pH, contact time, co-ions, adsorbent dose, and temperature	45.29	20–140	Electrostatic attraction	65
12	Nano-CS/Clino@PEHA	NO_3^-	277.77 mg g^{-1}	pH, co-existing ions, contact time, and adsorbent dose	30.24	100–300	Electrostatic attraction	77
13	Nano-CS/Clino@H		227.27 mg g^{-1}		33.46			
14	Nano-CS/Clino		185.18 mg g^{-1}		36.256			
15	Chitosan–polystyrene–Zn nanocomposite	NO_3^-	82.5%	pH and adsorbent dose	—	50	Electrostatic attraction	76
16	Chitosan/ZeoliteY/Nano ZrO_2 nanocomposite	NO_3^-	23.58 mg g^{-1}	pH, contact time, and adsorbent dose	54.619	5–200	Electrostatic attraction	87
17	CTsAl/f-MWCNTs	NO_3^-	96.8%	pH, contact time, and adsorbent dose	254.01	50	Electrostatic attraction	78
18	PAN/AC	NO_3^-	48.9 mg g^{-1}	pH, adsorbent dose, initial concentration, and temperature	260.5	25–75	Electrostatic attraction and ion exchange	73
19	MgAl-LDHs/SA	NO_3^-	22.36 mg g^{-1}	pH and co-existing ions	127.8	50–500	Electrostatic attraction and precipitation	88

© 2023 The Author(s). Published by the Royal Society of Chemistry

Open Access Article. Published on 30 Thang Mi 2023. Downloaded on 01/06/2026 7:15:53 CH.
This article is licensed under a Creative Commons Attribution-NonCommercial 3.0 Unported Licence.

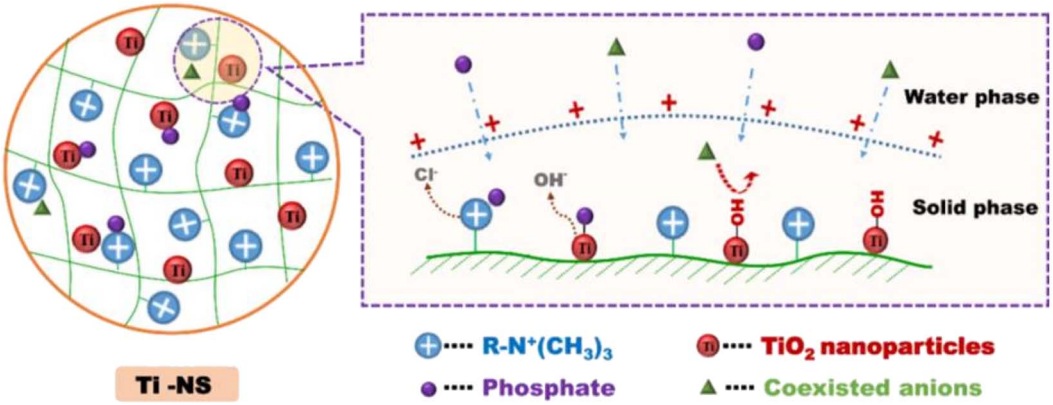

Fig. 2 Possible mechanism of phosphate removal by Ti-NS nanocomposite. Reproduced with permission from ref. 91 with permission from Elsevier, copyright 2019.

promising materials for the efficient recovery of PO_4^{3-} from wastewater which can be used as a fertilizer in soil amendments. Thus, the prevention of secondary pollution can be achieved by reusing the recovered nutrients for the intended purpose.[1]

2.2.1.1. Factors affecting the adsorption mechanism of phosphate. Polymeric nanocomposite adsorbents have a great ability to bind the PO_4^{3-} ion due to the presence of multiple active surfaces. For example, the triaminotriazine graphene oxide alginate (TATGO@Alg) composite beads contain several $-NH_2$ and –OH groups. The protonation of the $-NH_2$ and –OH groups at lower pH values assists in binding PO_4^{3-} ions *via* electrostatic attraction. The BET surface of alginate was found to be small (3.279 $m^2\ g^{-1}$), while TATGO@Alg composite beads exhibited improved surface area (45.29 $m^2\ g^{-1}$).[65] The increase in the surface area of alginate is due to the loading of the graphene oxide during composite formation. Thus, a larger surface area facilitated faster transfer of PO_4^{3-} ions.[86] Indeed, the amount of protonated amine groups is responsible for the binding of PO_4^{3-}. Thus, an increased protonated surface could be achieved by optimizing the pH of the solution. From this point of view, Nie's group proposed a possible adsorption mechanism of PO_4^{3-} on the quaternary amine polymer TiO_2 (Ti-NS) composite surface (Fig. 2). The Ti-NS composite possesses positively charged quaternary amine groups on the polymer. As a result, inner-sphere complexation with TiO_2 and electrostatic attraction by the quaternary ammonium groups on the composite surfaces enhance the uptake of PO_4^{3-}.[91] Apart from this, the electrostatic attraction between the PO_4^{3-} ion and the quaternary amine groups is a way to trap PO_4^{3-} by cross-linked chitosan (Fig. 7A).[92] In addition to complexation and electrostatic attraction between PO_4^{3-} and the surface of the adsorbent, precipitation occurring between PO_4^{3-} and dissolved cations like La^{3+} is also another mechanism of PO_4^{3-} recovery.[81]

In adsorption studies, the pH of a solution is a major parameter for the proper sorption of water contaminants, particularly PO_4^{3-} ion. The pH at which the adsorbent surface is electrically neutral is called the point of zero charges (pHpzc). Thus, the surface becomes positively charged below pHpzc, while it is negatively charged above pHpzc.[76] The lanthanum attapulgite chitosan (LaATP/CS-0.1) hydrogel bead revealed a maximum adsorption capacity (114.1 mg g^{-1}) at pH 6 while exhibiting a pHpzc of 8.96. Thus, the LaATP/CS-0.1 composite surface charge becomes positive below the pHpzc value, which leads to electrostatic attraction between PO_4^{3-} and the protonated surface.[93] However, the surface could be surrounded by OH^- ions, which leads to repulsion instead of attraction towards PO_4^{3-} above the pHpzc value.[65]

The adsorption of PO_4^{3-} could be achieved in a wide range of pH. For example, hydro-assisted synthesized zirconium alginate kaolinite (Zr@AlgKN) composite beads showed an increase in adsorption capacity towards PO_4^{3-} from pH 3–7 while the pHpzc value was 5.64.[86] Adsorbents like bimetallic lanthanum and iron hydroxide encapsulated chitosan (La/Fe–Cs) composites are effective in acidic mediums.[1] However, MgO lignin-based bio-charcoal (MFLC) revealed excellent removal efficiency (94.71%) towards PO_4^{3-} at a pH of 10, indicating that MFLC showed a better performance even in an alkaline solution.[82] This could be due to the phosphate species of $H_2PO_4^-$, HPO_4^{2-}, and PO_4^{3-} interacting differently in a wide pH range.[1,42] Thus, the occurrence of phosphate species assists the adsorbent surface in interacting in different pH ranges. In this regard, H_3PO_4 exists at pH $\leq$ 2 and $H_2PO_4^-$ (2.12–7.21), HPO_4^{2-} (7.21–12.67), and PO_4^{3-} ($\geq$12) (Fig. 3A) have pKa values of pK_1 = 2.12, pK_2 = 7.21, and pK_3 = 12.67, respectively, in the dissociation of phosphate species.[94] Thus, $H_2PO_4^-$ is the dominant species in acidic media, indicating adsorption is usually favourable at lower pH.[95]

Preparation of a material that can fit the purpose of the adsorption technique is very important. For example, lanthanum-chitosan treated with an optimum amount of glutaraldehyde as a cross-linking agent showed a better PO_4^{3-} adsorption capacity in a wide pH range (Fig. 3B). Also, the one-fold glutaraldehyde crosslinked La-CTS-1X composite showed better performance than the two-fold crosslinked La-CTS-2X.[96] The decrease in adsorption capacity with a high amount of crosslinker is due to the decrease in surface porosity.[97]

Open Access Article. Published on 30 Thang Mi 2023. Downloaded on 01/06/2026 7:15:53 CH.
This article is licensed under a Creative Commons Attribution-NonCommercial 3.0 Unported Licence.

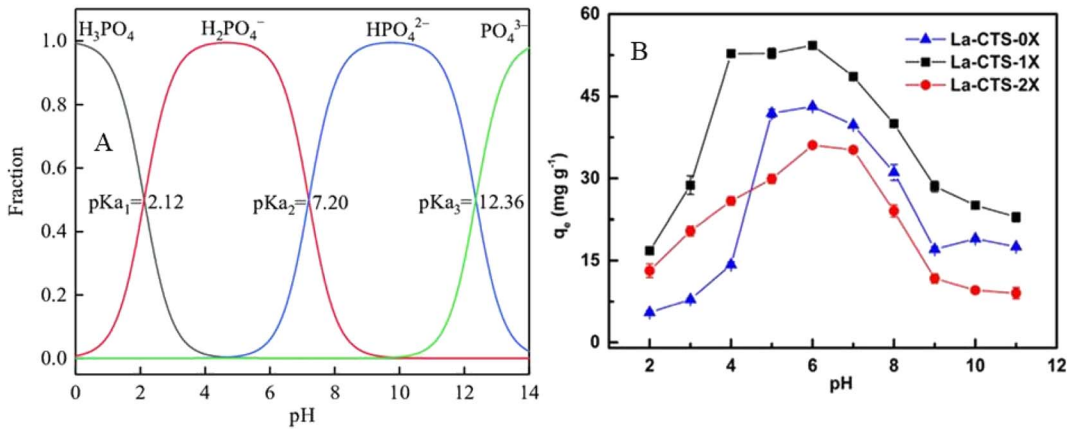

Fig. 3 (A) Phosphate species distribution at different pH values. Reproduced with permission from ref. 98 with permission from Elsevier, copyright 2022. (B) The effect of pH and amount of crosslinker on adsorption capacities of La-CTS towards PO_4^{3-}. Reproduced with permission from ref. 96 with permission from Elsevier, copyright 2020.

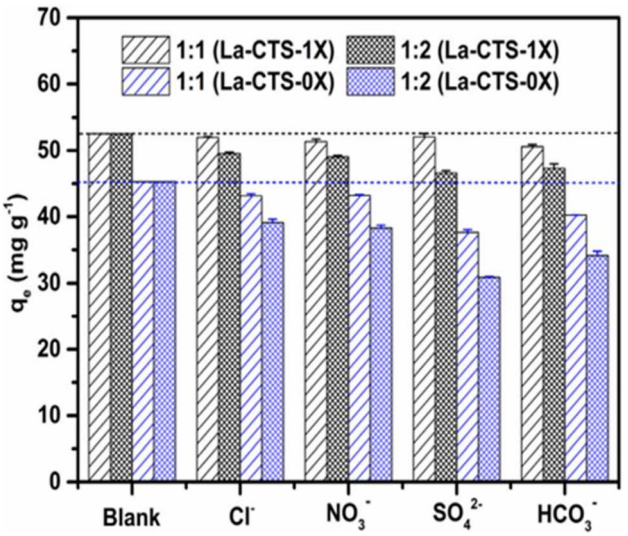

Fig. 4 Effect of coexisting ions on PO_4^{3-} recovery by La-CTS-1X and La-CTS-0X (the ratios of the initial PO_4^{3-} concentration to the coexisting ion concentration are 1 : 1 and 1 : 2). Reproduced with permission from ref. 96 with permission from Elsevier, copyright 2019.

Since the adsorption mechanism of adsorbent towards PO_4^{3-} is based on non-specific effects, some coexisting ions result in a decrease in the adsorption capacity by occupying the active adsorption sites.[96] The MgO-functionalized lignin-based bio-charcoal (MFLC) exhibits high adsorptive selectivity for PO_4^{3-} which is due to the selectivity of MgO in a composite towards PO_4^{3-} without a clear competing effect with other existing ions like HCO_3^-, NO_3^-, Cl^-, and SO_4^{2-}.[82] However, the most common interfering ion in the adsorption of PO_4^{3-} is SO_4^{2-}. During the adsorption of PO_4^{3-} by lanthanum-loaded cross-linked chitosan, the competition effect of SO_4^{2-} and Cl^- is high even though the material is selective towards PO_4^{3-} when compared to other co-existing ions like $HCrO_4^-$, HCO_3^-, and F^- (Fig. 4).[96] There is also a high interfering effect of SO_4^{2-} for adsorption of PO_4^{3-} over TATGO@Alg composite beads.[65] This could be due to the metallic surface of the composite having a comparable affinity towards PO_4^{3-} and other competing ions. Besides this, phosphate species other than PO_4^{3-} ($H_2PO_4^-$ and HPO_4^{2-}) could dominate other ions over a wide range of pH. Indeed, the interference of co-existing ions could be minimized by using material selective towards PO_4^{3-}. For example, lanthanum hydroxide loaded polyethyleneimine graft lignin (AL-PEI-La) nanocomposite had very good adsorption capacity in the presence of HCO_3^-, SO_4^{2-}, and NO_3^- and possessed good selectivity and affinity for PO_4^{3-}.[81]

Temperature is another important factor for optimum experimental conditions for the adsorption of PO_4^{3-}. In some cases, the adsorption of PO_4^{3-} increases with an increase in temperature. For example, the temperature of 313 K is considered the optimal temperature for PO_4^{3-} adsorption by MFLC,

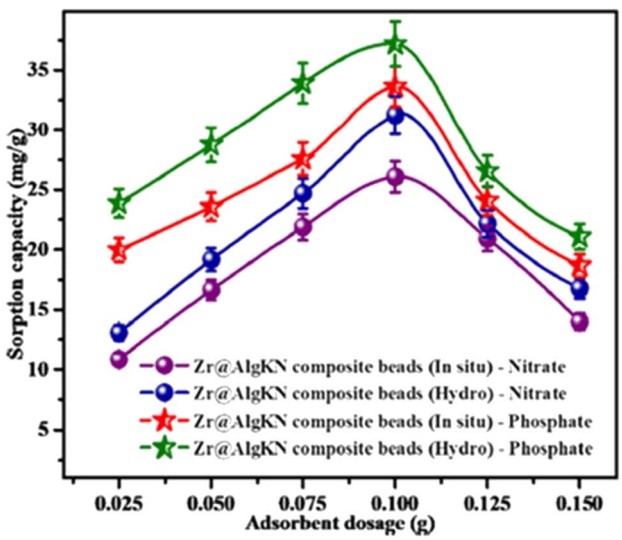

Fig. 5 Effect of adsorbent dose on adsorption capacity of *in situ* and hydrothermal synthesized Zr@AlgKN composite beads towards NO_3^- and PO_4^{3-}. Reproduced with permission from ref. 86 with permission from Elsevier, copyright 2020.

© 2023 The Author(s). Published by the Royal Society of Chemistry

Open Access Article. Published on 30 Thang Mi 2023. Downloaded on 01/06/2026 7:15:53 CH.
This article is licensed under a Creative Commons Attribution-NonCommercial 3.0 Unported Licence.

resulting in a removal efficiency of 98.54%.[82] At optimum temperature, the mobility of PO_4^{3-} ions increases and thus more ions interact with the active sites of the adsorbent.[81]

The adsorbent dosage is another key factor for the removal of PO_4^{3-}. When the adsorbent dosage increases, the active adsorptive sites also increase, which enhances adsorption capacity. From this perspective, the Zr@AlgKN composite achieved maximum adsorption capacity towards PO_4^{3-} at the optimum adsorbent dose of 0.1 g (Fig. 5).[86] However, a decrease in adsorption capacity after the optimum dosage is caused by the overlapping of the active sites of the surface. The 50% Fe_3O_4 anchored polyaniline graphene oxide ($Fe_3O_4$50%-PANI@GO) composite showed maximum adsorption capacity towards PO_4^{3-} (135.67 mg g^{-1}) using an adsorbent dose of 0.1 g.[85] However, the surface becomes saturated after the optimum adsorbent dose is applied and no further adsorption capacity was observed.

2.2.1.2. Adsorption isotherm and kinetics. Kinetics and isothermal studies are vital in adsorption to know the possible predominating adsorbate–adsorbent interaction. The experimental data for the adsorption of PO_4^{3-} by cross-linked lanthanum-chitosan fitted the Langmuir isotherm model (R^2 = 0.9998), confirming a homogeneous adsorption process and a monolayer formation process.[96] On the other hand, PO_4^{3-} adsorption on the TATGO@Alg composite was fitted with the Freundlich model, which indicates a multilayer heterogeneous surface during adsorption.[65] The maximum adsorption capacity of La/Fe–Cs composites towards PO_4^{3-} also fitted the Langmuir isotherm model (Fig. 6A).[1] Nevertheless, both single-layer and multilayer adsorption took place when different PNCs were employed for the removal of PO_4^{3-}.[86]

To investigate the kinetics of PO_4^{3-} adsorption, the TATGO@Alg composite beads were employed at temperatures of 303, 313, and 323 K. Thereafter, the pseudo-second-order model was found to be the best-fit model.[65] The pseudo-second-order was also suitable for the adsorption of PO_4^{3-} by $Fe_3O_4$50%-PANI@GO composite beads.[85] A higher R^2 value was obtained during the adsorption study of PO_4^{3-} by La/Fe–Cs composites, which suggests a pseudo-second-order kinetic model rather than a pseudo-first-order in PO_4^{3-} adsorption (Fig. 6B).[1] Thus, PNC adsorbents possess both pseudo-first-order and pseudo-second-order kinetic models, indicating all possible interactions attained on the surface. However, in most PNC adsorbents, pseudo-second-order kinetics were attained. This indicates that the chemisorption process is taking place due to the presence of an active functional surface when compared to the physisorption process.

2.2.1.3. Thermodynamic parameters. Together with kinetic and isothermal studies, thermodynamic parameters, such as standard enthalpy change (ΔH°), standard Gibbs free energy change (ΔG°), and standard entropy change (ΔS°), are essential to determining the mechanism of the adsorption process.[78] A positive ΔH° and a negative ΔG° often indicate favourable endothermic adsorption, while ΔS° shows increased randomness which could contribute to the adsorption process. A ΔH° greater than 25 kJ mol^{-1} and activation energy of 40 kJ mol^{-1} could indicate the presence of chemisorption.[99] For instance, the thermodynamic investigation of the adsorption of phosphate on TATGO@Alg composite revealed a negative ΔG° and positive ΔH°, indicating that PO_4^{3-} adsorption followed a spontaneous endothermic process. Further, the ΔS° is positive, which indicates an increase in the randomness of the process at the solid–liquid interface.[65] The increased entropy could be due to the external boundary layer diffusion of the adsorbate anions into the polymer matrix. This could be explained as the PO_4^{3-} molecules on the adsorbent surface replacing the water molecules.[100] Similarly, PO_4^{3-} adsorption on TATGO@CS composite beads exhibited a spontaneous endothermic process with an increase in entropy.[74] On the other hand, adsorption of PO_4^{3-} on crosslinked lanthanum–chitosan nanocomposite revealed ΔG°, ΔH°, and ΔS° values of −43.7 kJ mol^{-1}, −132 J mol^{-1} K^{-1}, and −4.60 kJ mol^{-1}, respectively. This indicates the system follows a spontaneous exothermic process with declining entropy.[96]

2.2.2. Recovery of nitrate and ammonia from wastewater by polymer-based nanocomposite materials. The disposal of nitrate and ammonia directly into the environment leads to the eutrophication of the aquatic environment, which results in ecological imbalance. Thus, different mitigation mechanisms, including adsorption, have been developed to overcome such

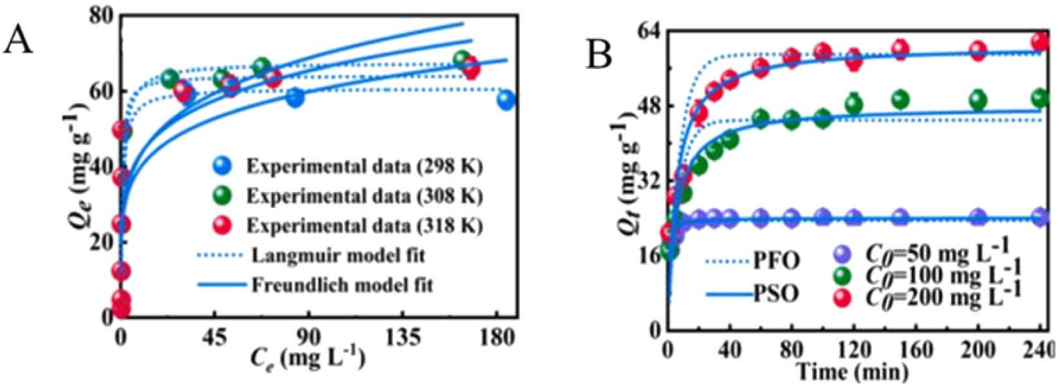

Fig. 6 (A) The Langmuir and Freundlich isotherm models and (B) pseudo-first-order and pseudo-second-order kinetics models for the adsorption of PO_4^{3-} on La/Fe–Cs composites. Reproduced with permission from ref. 1 with permission from Elsevier, copyright 2022.

Open Access Article. Published on 30 Thang Mi 2023. Downloaded on 01/06/2026 7:15:53 CH.
This article is licensed under a Creative Commons Attribution-NonCommercial 3.0 Unported Licence.

problems. Such techniques are helpful to prevent the release of excessive nitrogen from different sources to water bodies. This section gives insight into the adsorption mechanisms and affecting parameters and factors of PNC adsorbents for the recovery of nitrate and ammonia from wastewater.

2.2.2.1. Factors affecting the adsorption mechanism and efficiency. Surface functionalization of the adsorbent is a way to enhance the adsorption capacity. In this case, the increase of active sites of PNC enhances the electrostatic attraction between the surface and NO_3^- ions. This is due to the presence of the positively charged $-NH_2$ and –OH adsorbent sites that trap NO_3^-.[77] Hydrothermally synthesized Zr@AlgKN composite beads with a surface area of 78.93 $m^2\ g^{-1}$ have been studied for their strong affinity towards NO_3^-. Furthermore, the electrostatic attraction of NO_3^- in solution is strong towards the protonated $Zr–O–OH_2^+$.[86] The higher surface area (45.29 $m^2\ g^{-1}$) of TATGO@Alg composite beads exhibited strong trapping of NO_3^-. Indeed, the functionalized surface of TATGO@Alg composite in the form of amine-rich acetamide ($–CONH_2$) leads to strong attraction of NO_3^-.[65] Further, the protonated amino groups on a polymer like chitosan are the main trapping sites for the anionic nutrients $N–NO_2$ and $N–NO_3$ in acidic medium. Thus, $–NH_3^+$ electrostatically attracts the negatively charged nitrite and nitrate (Fig. 7B and C). In addition, the hydrogen bond formation between the oxygen atom of the anion and the hydrogen atom from either the ammine or hydroxyl group of chitosan further enhances the sorption process.[92]

The pH of a solution is a key parameter for the recovery of nitrate and ammonia using PNC. Thus, the level of NO_3^- adsorption depends on having a pH that exhibits a positively charged functional group for the enhancement of interaction. A chitosan–polystyrene–Zn (Ch–ps–Zn) composite removed 90% of the NO_3^- ions using 0.5 g adsorbent at a pH of 3 with a contact time of 30 min.[76] Similarly, the protonation of $–NH_2$ groups from chitosan significantly affects and causes an increase in the electrostatic attractions between the positively charged chitosan alumina functionalized multiwalled carbon nanotube (CTsAl/f-MWCNTs) composite surface and negatively charged NO_3^- at pH 2–6.[78] Cobalt oxides and magnetic nanoparticles doped with polyaniline (PANI-Co_3O_4@MNPs) removed 68.97 mg g^{-1} of NO_3^- at pH 6 using 0.06 g adsorbent.[71]

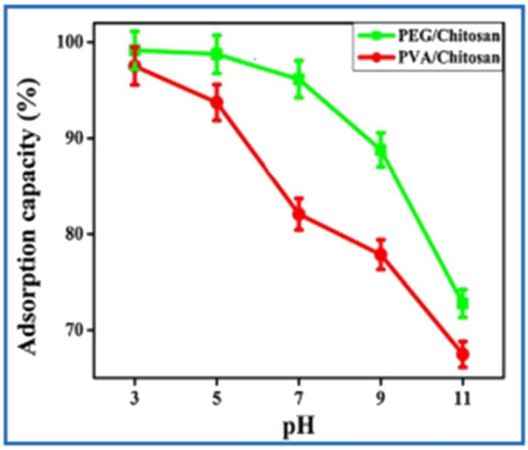

Fig. 8 Effect of pH on adsorption of NO_3^- by PEG/Cs and PVA/Cs. Reproduced from ref. 101 with permission from Elsevier, copyright 2016.

The maximum NO_3^- removal occurred at a pH of 4 when iron oxide poly(methacrylic acid)-*block*-poly(*N*-isopropylacrylamide) (P(MAAc-*b*-NIPAM)/Fe_3O_4) nanocomposite was used as adsorbent. The polyethylene glycol chitosan (PEG/Cs) and polyvinyl alcohol chitosan (PVA/Cs) composite removed 50.68 and 35.03 mg g^{-1} of NO_3^-, respectively, at pH 3 (Fig. 8).[101] Thus, through increasing pH, there is a slight decrement in the removal efficiency which indicates that lower pH is favourable for the uptake of NO_3^- by PNC adsorbents.[102] In the recovery of NH_4^+-N, 64.6% efficiency was obtained when chitosan films alone were used as adsorbents, whereas the efficiency increased to 98.05% when modified chitosan film using nanoclay was applied at a pH of 6.[103]

The adsorption of NO_3^- by PNC materials is time-dependent, and in most cases the maximum adsorption was attained in a short time. According to Kumar and Viswanathan, (Hydro) Zr@AlgKN composite beads exhibited an adsorption capacity of 31.24 mg g^{-1} toward NO_3^- with an equilibrium time of

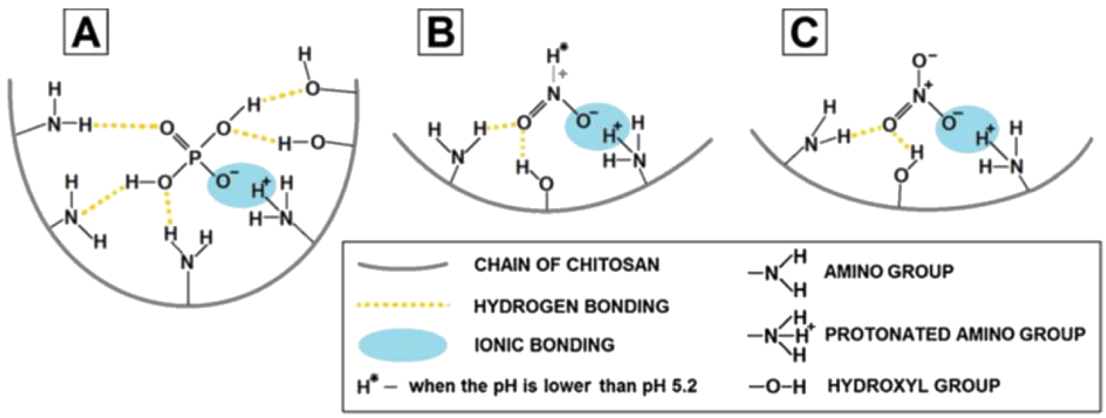

Fig. 7 Possible mechanisms of nutrient bonding onto chitosan sorbents: (A) PO_4^{3-}, (B) $N–NO_2$, and (C) $N–NO_3$. Reproduced with permission from ref. 92 with permission from Elsevier, copyright 2017.

© 2023 The Author(s). Published by the Royal Society of Chemistry

Open Access Article. Published on 30 Thang Mi 2023. Downloaded on 01/06/2026 7:15:53 CH.
This article is licensed under a Creative Commons Attribution-NonCommercial 3.0 Unported Licence.

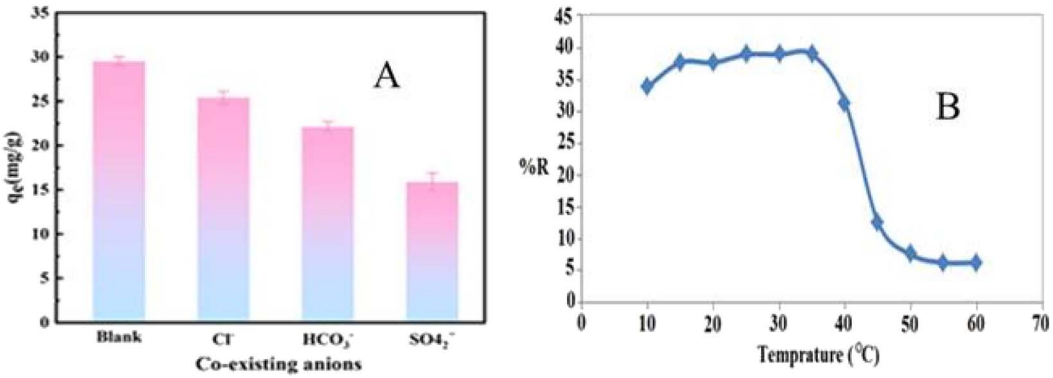

Fig. 9 (A) Effect of co-existing ions on NO_3^- adsorption onto GCS@LDH. Reproduced with permission from ref. 104 with permission from Elsevier, copyright 2022. (B) The temperature effect on the adsorption of NO_3^- onto CTS/ZY/ZrO_2 nanocomposite. Reproduced with permission from ref. 87 with permission from Elsevier, copyright 2016.

30 min.[86] In another study, a fast uptake of NO_3^- by CTsAl/f-MWCNTs adsorbents was also observed within the first 30 min.[78] The NO_3^- removal efficiency of P(MAAc-*b*-NIPAM)/Fe_3O_4 increased from 67.05 to 74.28% when contact time increased, but gradually declined after 40 min, which is taken as equilibrium contact time.[102] The fast adsorption attained could be due to the porosity and functionality of PNC adsorbents.

The presence of interfering ions like HCO_3^-, SO_4^{2-}, F^-, Cl^-, and $HCrO_4^-$ also affects the efficiency of PNC. For example, $HCrO_4^-$ did not show a significant effect on the adsorption capacity of Zr@AlgKN composite towards NO_3^-, while Cl^- and F^- competed slightly, and SO_4^{2-} affected the adsorption capacity.[86] Similar effects also occurred in the adsorption of NO_3^- by TATGO@Alg composite beads.[65] The adsorption of NO_3^- on polyaniline activated carbon (PANI/AC) composite is affected by the presence of CO_3^{2-} ion.[73] Moreover, the adsorption capacity of core–shell chitosan layered double hydroxide (GCS@LDH) composite for NO_3^- decreased (Fig. 9A) due to co-existing ions (Cl^-, HCO_3^-, and SO_4^{2-}) which competed for the active sites of the composite surface.[104] The negative effect of oxyanions (SO_4^{2-} and CO_3^{2-}) on the adsorption of NO_3^- could be due to the stronger electrostatic attraction between the high valence anion and the adsorbent under similar conditions.[73,105]

Temperature has a significant effect on adsorption experiments. A decrease in temperature brings an increase in the adsorption capacity in the recovery of NO_3^-. In most cases, the mobility of ions decreases at a lower temperature, which helps keep them trapped on the surface of the adsorbent.[77] The removal efficiency of chitosan/zeoliteY/ZrO_2 (CTS/ZY/ZrO_2) nanocomposite towards NO_3^- increased from 35 to 40% by increasing the temperature from 10 to 35 °C. However, the adsorption capacity decreased strongly in the temperature range of 40–50 °C (Fig. 9B).[87] In contrast, the PANI/AC composite showed comparable adsorption capacity in a varied temperature range,[73] indicating that the sorption process needs the proper selection of temperature-resistant material.

When the adsorbent dosage increased, the adsorption capacity also increased until the active sites of the surface became saturated. For example, the adsorption capacity towards NO_3^- increased until 0.1 g of Zr@AlgKN composite beads were used (Fig. 5).[86] According to Keshvardoostchokami *et al.*, 0.5 g of Ch–ps–Zn nanocomposite removed 97% of 10 mg L^{-1} of NO_3^-.[76] With an increase in the adsorbent dose from 0.03–0.14 g L^{-1}, the adsorption efficiency of NO_3^- by P(MAAc-*b*-NIPAM)/Fe_3O_4 superparamagnetic nanocomposite was increased from 70.89 to 73.95% and the optimum adsorbent dose was found to be 0.08 g L^{-1}.[102] Additionally, the PEG/Cs and PVA/Cs composite revealed a maximum adsorption capacity at a dose of 0.3 g (Fig. 10A), and no further increment was observed due to the overlapping of the active surface.[101]

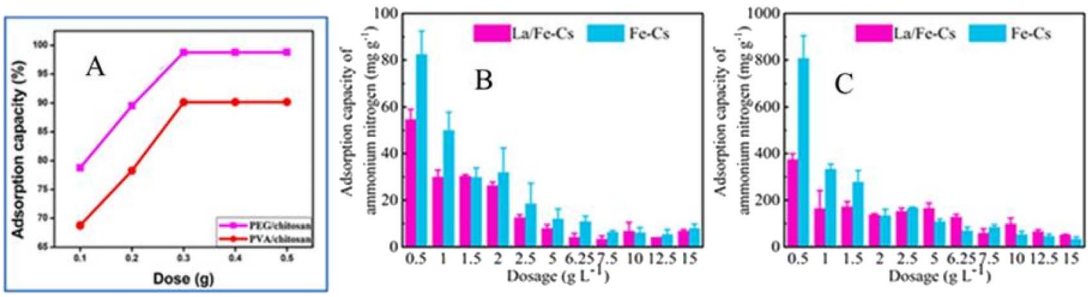

Fig. 10 (A) The effect of PEG/chitosan and PVA/chitosan composite dose on NO_3^- adsorption[101] with permission from Elsevier, copyright 2016. (B) The effect of Fe–Cs and La/Fe–Cs composite dose on ammonium–nitrogen removal from cow breeding wastewater and (C) pig farm wastewater. Reproduced with permission from ref. 1 with permission from Elsevier, copyright 2022.

Open Access Article. Published on 30 Thang Mi 2023. Downloaded on 01/06/2026 7:15:53 CH.
This article is licensed under a Creative Commons Attribution-NonCommercial 3.0 Unported Licence.

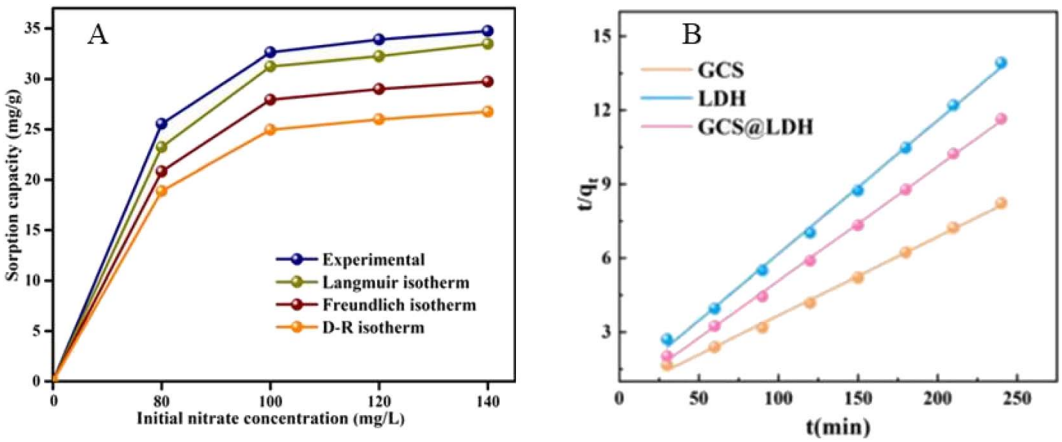

Fig. 11 (A) Experimentally measured isotherms for NO_3^- adsorption by Zr@AlgKN composite beads. Reproduced with permission from ref. 86 with permission from Elsevier, copyright 2020. (B) Pseudo-second-order model on NO_3^- removal by GCS, LDH, and GCS@LDH. Reproduced with permission from ref. 104 with permission from Elsevier, copyright 2022.

Similarly, a 0.025–0.150 g dose of TATGO@Alg composite beads showed an increase in adsorption capacity (23.24 to 52.08 mg g^{-1}) towards NO_3^-.[65] However, the adsorption efficiency decreased after the optimum dose. This indicates that a small amount of PNC adsorbents have high efficiency in NO_3^- recovery from wastewater. Similarly, in the removal of NH_4^+ by chitosan–bentonite film composite, the adsorption efficiency increased until the optimum adsorbent dose was used.[103] Fe–Cs and La/Fe–Cs composites showed significant adsorption efficiency towards ammonium–nitrogen, although the adsorption efficiency decreased when the adsorbent dosage was increased in cow breeding farm wastewater (Fig. 10B) and pig farm wastewater (Fig. 10C).[1]

2.2.2.2. Adsorption isotherm and kinetics. The isotherm studies explained the relationship between the amount of NO_3^- adsorbed and the equilibrium concentration of the solution. Thus, adsorption isotherms are helpful to investigate the type of adsorption that takes place on the surface of the adsorbents. The Langmuir isotherm fitted better for NO_3^- adsorption on the Zr@AlgKN composite beads adsorbent, indicating a single layer type of adsorption takes place (Fig. 11A).[86] However, the adsorption of NO_3^- by functionalized nano-CS/Clino@PEHA and nano-CS/Clino@H was fitted with the Freundlich isotherm.[77] Adsorption of NO_3^- on CTsAl/f-MWCNTs adsorbents also fitted well in the Freundlich model, which indicates that the adsorption process of NO_3^- is a multilayer formation on the heterogonous surface.[78] Either a single-layer homogenous surface or multilayer heterogeneous surface could be formed based on the interaction of NO_3^- and adsorbent.

Kinetics studies are also helpful for the design of adsorption systems and the evaluation of adsorption efficiency. It is possible to identify the adsorption interaction between the adsorbate and the adsorbent surface. In a kinetic study of the adsorption of NO_3^- by TATGO@Alg composite beads, the pseudo-second-order model was the best-fitted model.[65] According to Kumar and Viswanathan, the adsorption of NO_3^- by Zr@AlgKN composite beads also fitted with the pseudo-second-order model, in which chemisorption occurred.[86] Similarly, the adsorption of NO_3^- on GCS@LDH fitted with the pseudo-second-order model, indicating that a chemisorption process takes place on the surface (Fig. 11B).[104] Nevertheless, both physisorption and chemisorption can take place based on the nature of the adsorbent.[77]

2.2.2.3. Thermodynamic parameters. Thermodynamics is used to describe the adsorption properties of NO_3^- by the adsorbent. According to Kumar and Viswanathan, a thermodynamic study on the removal of NO_3^- by Zr@AlgKN composite beads revealed a negative ΔG° value, indicating that NO_3^- adsorption is spontaneous. Likewise, positive ΔH° indicates that heat energy is absorbed and the adsorption is endothermic, while positive ΔS° indicates the randomness of surface interaction.[86] Similarly, other PNC adsorbents, like PEG/Cs and PVA/Cs composite,[101] chitosan and zeolite nano-CS/Clino@PEHA,[77] and CTsAl/f-MWCNTs adsorbents,[78] follow spontaneous thermodynamic processes while attaining an endothermic process and randomness on the surface whenever employed as an adsorbent for recovery of NO_3^-.

2.2.3. Reusability of polymer-based nanocomposite adsorbents. In addition to adsorption performance, adsorbents must possess a recyclable character, which is a key factor in evaluating their stability in practical applications. Due to their mechanical strength and stability, PNC materials can be regenerated by following an appropriate desorption procedure. Thus, better acid–alkaline resistance of PNC adsorbents assists them in retaining their original adsorption efficiency.[73] For example, a removal efficiency greater than 70% for up to six regeneration cycles was obtained by TATGO@Alg composite beads for NO_3^- removal from wastewater.[65] The NO_3^- adsorption capacity remained stable for 10 cycles, while the PO_4^{3-} uptake decreased with the initial cycle and cycles 4–10 for the simultaneous adsorption of NO_3^- and PO_4^{3-} by triethylamine functionalized polystyrene encapsulated with Fe(III) hydroxide (HFO@TPR).[106] Similarly, regeneration was achieved for up to four cycles for Zr@AlgKN composite beads and the decline in

© 2023 The Author(s). Published by the Royal Society of Chemistry

Open Access Article. Published on 30 Thang Mi 2023. Downloaded on 01/06/2026 7:15:53 CH.
This article is licensed under a Creative Commons Attribution-NonCommercial 3.0 Unported Licence.

adsorption efficiency was 98–75%. The decrease in the efficiency of the adsorbent during regeneration is due to the competing effect of alkaline OH^- ions.[86] The MFLC also attained a removal efficiency of 72.01% of its original performance after six cycles of reuse.[82] Thus, PNC adsorbents could be promising candidates for nutrient recovery.

3. Resource recovery and its applications

The recovery of nutrient resources has dual functionality. The first is pollution prevention in water bodies by creating a clean and conducive aquatic environment and the second is applying the recovered resource in a useful form to prevent secondary pollution. In this regard, it is possible to use recovered nutrient resources as fertilizer. For example, phosphate adsorbed on eggshell and rice straw CaO–biochar composite was applied as a fertilizer to improve soil fertility.[34] The MgAl LDHs/sodium alginate (MgAl-LDHs/SA) beads were found to greatly enhance the soil's water retention capacity through nitrate release after adsorption.[88] The effect of phosphate-laden-Mg/NBC as a slow-release fertilizer was checked by a pot test. Compared with the controls, 5 and 10% improvements were obtained in the growth of beans and garlic, respectively.[33] Similarly, the magnetic lignin–polyethyleneimine nanocomposite biosorbent recovered 43 mg g^{-1} phosphorous from an aqueous solution and was used as a fertilizer in seed germination and a seedling growth study. The recovered P-laden lignin fertilizer significantly improved both the shoot length and diameter (14.98 cm and 2.01 mm) when compared to the control groups (9.84 cm and 1.81 mm).[84]

Slow-release behaviour and water retention capacity are important parameters of the material in the delivery of spent nutrients to the soil. According to Vu and Wu, nutrient-laden MgAl-LDHs/SA beads showed a higher release percentage (~90% after 40 days and 6 days for beads and milled beads, respectively) for NO_3^- adsorbed from groundwater. In addition, MgAl-LDHs/SA beads showed a good water retention capacity (820 ± 15% after 47 days) at pH 7, which does not disturb the natural soil pH.[88] Thus, water retention capacity is an essential property for fertilizer usage in the dry season. However, water swelling during adsorption is not favoured and could reduce the adsorption capacity of PNCs. Thus, some PNCs showed swelling properties during the recovery of nutrients; however, the adsorption could be completed in a few hours and did not significantly affect the sorption process,[107] while the swelling property during the slow release process could take place over several days or even a month.

Sorbent–nutrient interaction is another important property for the slow-release behaviour of recovered nutrient resources. For example, the PO_4^{3-} recovered by dolomite alginate (DA) composite exhibited a slow release process (90% PO_4^{3-} release within 60 days) due to the formation of Ca and Mg phosphate precipitate.[108] Apart from this, the type of soil is a determining factor for the effective and sustainable release of fertilizer. Soil that has low clay content is vulnerable to leaching and loss of nutrient enrichment.[109] Thus, coating the released fertilizer with polymer hybrid materials such as cellulose biochar composite could reduce the leaching of nutrients up to 43.90% within 80 days.[110] Indeed, the selection of cost-effective and non-toxic adsorbent material is vital for the initiative of a circular economy through the proper recovery of nutrient resources from wastewater which finally could be used for fertilizer.

4. Potential impacts of polymer-based nanocomposite adsorbents on ecological systems

Polymer-based nanocomposite adsorbents are the most efficient materials to recover nutrient resources from wastewater. However, in some cases, a composite material released into the environment could have a toxicological impact on the living organism. The toxicity of nanocomposites arises from their physicochemical characteristics like size, morphology, amount, bioaccumulation, solubility, biodegradability, and agglomeration effect.[111] These nanoparticles can accumulate in organ systems like the heart, liver, kidney, and brain after inhalation, ingestion, or skin contact with living things.[112] Once the nanoparticles enter the biological system, they can interact with cells and produce reactive oxygen species. This process continues to break peptide bonds in DNA and interfere with the function of proteins if it is not defended by antioxidant activity. Such a mismatch in the metabolic process results in inflammation, oxidative stress, oxidative damage to biomolecules, and finally cell death.[113]

Nowadays, the toxicity effects of nano-level engineered materials are reported. Karkossa *et al.* studied the different levels of oxidative stress in rats caused by SiO_2 and TiO_2 nanomaterials. Inflammation and oxidative stress were observed in the *in vivo* and *in vitro* studies.[114] Further, high mortality of zebrafish embryos occurred at 10 mg L^{-1} exposure to CuO nanoparticles. CuO nanoparticles in low ionic strength exhibited higher toxicity, abnormal heartbeat, and deformation of zebrafish embryos.[115] Zebrafish died completely in 96 h at 0.1 mg L^{-1} exposure to ZnO nanoparticles. However, developmental toxicity slightly decreased through the doping of the more toxic ZnO nanoparticles with less toxic TiO_2, which may be due to the shape change during doping.[116] Polyethylene nanoplastic also negatively affects the cardiac output and blood circulation of zebrafish when the dose is above 0.05 mg L^{-1}.[117]

PNC does not show toxicity effects on living organisms. In fact, PNC materials, particularly natural polymers, can be employed as drug-delivering agents. For example, Ouyang and colleagues synthesized a Puerarin@Chitosan (P@C) composite for infected bone repair. The chitosan in P@C acts as a bacterial membrane-destroying agent, and the puerarin is used as a bioactive ingredient. As a result, the P@C composite revealed good inhibition of *Escherichia coli* during the *in vivo* study on infected rats.[118] Bacterial nanocellulose was also employed as a virus antigen carrier for vaccination and an improvement in immune-related genes was observed.[119] Additionally, chitosan-based materials have been used for different medical

Open Access Article. Published on 30 Thang Mi 2023. Downloaded on 01/06/2026 7:15:53 CH.
This article is licensed under a Creative Commons Attribution-NonCommercial 3.0 Unported Licence.

purposes like wound healing,[120] drug delivery,[121] and anticancer activity.[122] Nevertheless, it is difficult to conclude that polymers are always non-toxic. For example, cellulose nanocrystals from different sources did not show developmental or mortality effects on zebrafish, but some oxidative stress at a 0.01 mg L^{-1} dose was observed.[123] Comparatively, the metal and metal oxide nanoparticles cause significant toxicity due to their physicochemical properties.

5. Applicability of polymer-based nanocomposite adsorbents in recovery of nutrient resources from real wastewater

The recovery of nutrient resources from actual nutrient-rich water using PNC adsorbents has its own merits and demerits regarding their efficiency, which is impacted by different factors. In this regard, PNC adsorbents work in a wide range of pH. For example, the bimetallic La/Fe–Cs composites revealed an adsorption capacity of 67.52 mg g^{-1} of PO_4^{3-} with a removal efficiency of 63–95% in a pH range of 3–10 from eutrophic water sampled from a lake located in China.[1] Similarly, the polyaniline magnetic cobalt oxide nanocomposite (PANICo_3O_4@MNPs) removed 68.96 mg g^{-1} of NO_3^- from groundwater with a removal efficiency of 95.24% at pH 6, although the adsorption is unfavorable in alkaline medium.[71]

According to Kong *et al.*, the LaATP/CS-0.1 hydrogel bead was employed in domestic sewage and reduced the concentration of PO_4^{3-} from 18.95 to 3.57 mg L^{-1}.[93] The lanthanum oxide aegle marmelos and chitosan composite beads (La_2O_3AM@CS) also reduce the concentrations of NO_3^- and PO_4^{3-} from 17.59 and 26.04 mg L^{-1} to almost zero for a water sample collected from the Dindigul district, India. The La_2O_3AM@CS composite beads removed 27.84 and 34.91 mg g^{-1} of NO_3^- and PO_4^{3-}, respectively, from synthetic wastewater and thus showed good efficiency for a field water sample with a pH of 5.85, Cl^- of 380 mg L^{-1}, total hardness of 568 mg L^{-1}, and total dissolved solids of 439 mg L^{-1},[124] which are the most common natural constraints in the adsorption of nutrient resources from real wastewater.

Zirconium encapsulated chitosan quaternized (Zr@CSQ) beads were deployed in a wastewater sample collected from the Dindigul district and reduced the concentrations of NO_3^- and PO_4^{3-} from 16.56 and 20.11 mg L^{-1} to zero. Additionally, the Zr@CSQ beads simultaneously reduced the concentration of Cl^- from 476 to 289 mg L^{-1} and the total hardness from 756 to 465 mg L^{-1}.[125] The presence of cations (Mg^{2+} and Ca^{2+}) in the groundwater assists the adsorption process through precipitate formation with PO_4^{3-} ions.[126] Indeed, the distribution of phosphate species in a wide pH range also assists the applicability of PNCs in real wastewater.[94]

Despite their advantages, PNC adsorbents have limitations regarding their adsorption efficiency when they are employed in actual wastewater. Real polluted water usually contains coexisting interfering ions and dissolved solids that could negatively affect the sorption process of nutrient resources.[127] The active sites of the adsorbent can be locked by total organic carbon and other dissolved solids.[128] Thus, using PNC adsorbents with better selectivity towards the adsorbate is crucial in the recovery of nutrient resources from real wastewater. For example, the presence of Zr^{4+} in polyethylene glycol-modified *N*-isopropylacrylamide/sodium alginate zirconium (PNIPAM/SA-Zr) composite presented better selectivity and sorption capacity towards PO_4^{3-}.[126]

The $La(OH)_3$/porous carbon composites derived from alginate xerogel also showed better selectivity towards PO_4^{3-} in synthetic mixed coexisting anions at concentrations of 10–200 mg L^{-1}.[129] Further, the PNC adsorbents engineered with LDHs exhibited good adsorption capacity towards adsorbates in a wide pH range due to their buffering capacity.[88] Moreover, PNCs fabricated from two different polymers like chitosan and alginate exhibit good adsorption capacity in a wide pH range due to their basic and acidic natures, respectively.[107] Nonetheless, some PNCs are effective in acidic solutions only,[126] while others are effective in a wide pH range for the adsorption of anionic nutrients.[88,107] Thus, more exploration and modification are needed to improve the efficiency of PNCs in a wide pH range, which is crucial for their deployment in real wastewater.

6. Conclusions and future outlook

Given their unique properties, PNC adsorbents have received much attention for resource recovery from wastewater. The attractive features of PNC materials, particularly the biopolymers, are their availability, renewability, functionality, nontoxicity, and biodegradability. On the other hand, synthetic polymers like polyethylene exhibited better stability, though they are nonbiodegradable. Electrostatic attraction and ion exchange are the dominant mechanisms in recovering nutrient resources using PNC adsorbents. The adsorption of nutrient resources by PNC is highly dependent on pH, adsorbent dose, and coexisting ions. The kinetics of PNC for recovery of different nutrient resources from wastewater were fast. PNC has a high adsorption capacity with better stability than the pristine ones due to the various surface interactions between the adsorbent and adsorbate.

Although much literature is available on the utilization of PNC adsorbents for resource recovery, there is a large gap to be bridged. Particularly, due consideration has to be given to the fabrication of stable and low-cost PNC adsorbents. Although various adsorbents are available for the recovery of nutrients, the necessity of novel adsorbents with better performance has not been fulfilled. Several findings have been reported on the functionality and trapping mechanisms of PNC adsorbents towards nutrients. However, pilot scale studies and natural constraints like the performance of PNC in different seasons at different temperature ranges have not been reported. In addition, intensive exploration of the development of adsorbents for the simultaneous recovery and application of recovered nutrient resources as fertilizer needs further investigation using a standard approach.

© 2023 The Author(s). Published by the Royal Society of Chemistry

Open Access Article. Published on 30 Thang Mi 2023. Downloaded on 01/06/2026 7:15:53 CH.
This article is licensed under a Creative Commons Attribution-NonCommercial 3.0 Unported Licence.

Author contributions

Ahmed AM contributed in conceptualization, writing – original draft, and writing – review and editing. Mekonnen ML and Mekonnen KN contributed in the conceptualization, supervision, and writing – review and editing.

Conflicts of interest

The authors declare no known competing financial interests or personal relationships that could have appeared to influence the work reported in this paper.

Acknowledgements

The authors are grateful to Addis Ababa Science and Technology University Department of Industrial Chemistry for facility support.

References

1 G. Wang, X. Yue, S. Zhang, Q. Geng, J. Zheng, X. Xu, T. Li, Y. Pu, Y. Li and Y. Jia, *J. Cleaner Prod.*, 2022, **379**, 134833.
2 W. A. Wurtsbaugh, H. W. Paerl and W. K. Dodds, *Wiley Interdiscip. Rev.: Water*, 2019, **6**, e1373.
3 G. H. van der Lee, R. C. Verdonschot, M. H. Kraak and P. F. Verdonschot, *Limnologica*, 2018, **72**, 28–31.
4 E. M. Ali and H. M. Khairy, *Environ. Pollut.*, 2016, **216**, 437–449.
5 M.-P. Soro, K. M. N'goran, A. A. Ouattara, K. M. Yao and T. Diaco, *Mar. Pollut. Bull.*, 2023, **186**, 114391.
6 D. Tibebe, Y. Kassa, A. Melaku and S. Lakew, *Microchem. J.*, 2019, **148**, 374–384.
7 USEPA, *Effluent Standards and Limitations for Phosphorus*, US, 2011, **https://www.epa.gov/sites/default/files/2014-12/documents/wiwqs-nr217.pdf**, accessed on October 2023.
8 USEPA, *Nutrient control design manual*, US, 2010, **https://www.epa.gov/sites/default/files/2019-02/documents/nutrient-control-design-manual.pdf**, accessed on October 2023.
9 A. A. Ansari, G. S. Singh, G. R. Lanza and W. Rast, *Eutrophication: causes, consequences and control*, Springer, 2010.
10 C. Le, Y. Zha, Y. Li, D. Sun, H. Lu and B. Yin, *Environ. Manage.*, 2010, **45**, 662–668.
11 E. Daneshvar, C. Santhosh, E. Antikainen and A. Bhatnagar, *J. Environ. Chem. Eng.*, 2018, **6**, 1848–1854.
12 N. Jeke and F. Zvomuya, *Soil Sci. Soc. Am. J.*, 2018, **82**, 1004–1012.
13 Q. Gao, C.-Z. Wang, S. Liu, D. Hanigan, S.-T. Liu and H.-Z. Zhao, *Chem. Eng. J.*, 2019, **355**, 238–246.
14 T. Mkilima, T. Bazarbayeva, K. Assel, N. N. Nurmukhanbetova, I. B. Ostretsova, A. S. Khamitova, S. Makhanova and S. Sergazina, *Water*, 2022, **14**, 2929.
15 K. Y. Cheng, A. H. Kaksonen and G. B. Douglas, *Bioresour. Technol.*, 2014, **172**, 373–381.
16 J. Ano, B. G. H. Briton, K. E. Kouassi and K. Adouby, *J. Environ. Chem. Eng.*, 2020, **8**, 104292.
17 T. Nur, M. Johir, P. Loganathan, T. Nguyen, S. Vigneswaran and J. Kandasamy, *J. Ind. Eng. Chem.*, 2014, **20**, 1301–1307.
18 M. R. Awual, A. Jyo, S. A. El-Safty, M. Tamada and N. Seko, *J. Hazard. Mater.*, 2011, **188**, 164–171.
19 X. Li, Y. Peng, J. Zhang and R. Du, *Chem. Eng. J.*, 2021, **425**, 131449.
20 X. Luo, Q. Yan, C. Wang, C. Luo, N. Zhou and C. Jian, *Int. J. Environ. Res. Public Health*, 2015, **12**, 11975–11987.
21 Y. Lei, E. Geraets, M. Saakes, R. D. van der Weijden and C. J. Buisman, *Water Res.*, 2020, **169**, 115207.
22 C. Algieri, V. Pugliese, G. Coppola, S. Curcio, V. Calabro and S. Chakraborty, *Groundwater for Sustainable Development*, 2022, p. 100815.
23 R. R. Karri, J. N. Sahu and V. Chimmiri, *J. Mol. Liq.*, 2018, **261**, 21–31.
24 M. B. Bahrodin, N. S. Zaidi, N. Hussein, M. Sillanpää, D. D. Prasetyo and A. Syafiuddin, *Curr. Pollut. Rep.*, 2021, **7**, 379–391.
25 L. Rizzo, S. Malato, D. Antakyali, V. G. Beretsou, M. B. Đolić, W. Gernjak, E. Heath, I. Ivancev-Tumbas, P. Karaolia and A. R. L. Ribeiro, *Sci. Total Environ.*, 2019, **655**, 986–1008.
26 A. Khan, S. Malik, N. Ali, M. Bilal, M. El-Shazly and H. M. Iqbal, in *Sorbents materials for controlling environmental pollution*, Elsevier, 2021, pp. 463–491.
27 M. Peyravi and H. Rezaei, in *Metals in Water*, Elsevier, 2023, pp. 331–351.
28 Y. Öztürk and Z. Ekmekçi, *Miner. Eng.*, 2020, **159**, 106613.
29 D. de Haas, M. C. Wentzel and G. Ekama, *Water SA*, 2000, **26**, 439–452.
30 S. Pulkka, M. Martikainen, A. Bhatnagar and M. Sillanpää, *Sep. Purif. Technol.*, 2014, **132**, 252–271.
31 D.-W. Gao and Y. Tao, *Appl. Microbiol. Biotechnol.*, 2011, **91**, 887–894.
32 X. Luo, X. Wang, S. Bao, X. Liu, W. Zhang and T. Fang, *Sci. Rep.*, 2016, **6**, 1–13.
33 G. Begna Sisay, T. Belege Atisme, Y. Admassu Workie, Z. Worku Negie and M. Leul Mekonnen, *Environ. Nanotechnol., Monit. Manage.*, 2023, 19.
34 X. Liu, F. Shen and X. Qi, *Sci. Total Environ.*, 2019, **666**, 694–702.
35 Y. Deng, M. Li, Z. Zhang, Q. Liu, K. Jiang, J. Tian, Y. Zhang and F. Ni, *J. Environ. Chem. Eng.*, 2021, **9**, 105079.
36 M. Du, Y. Zhang, Z. Wang, M. Lv, Q. Xu, Z. Chen, Q. Wen and A. Li, *Sep. Purif. Technol.*, 2022, **298**, 121585.
37 O. Alagha, M. S. Manzar, M. Zubair, I. Anil, N. D. Mu'azu and A. Qureshi, *Nanomaterials*, 2020, **10**, 1361.
38 K. Wu, Y. Li, T. Liu, Q. Huang, S. Yang, W. Wang and P. Jin, *Appl. Surf. Sci.*, 2019, **478**, 539–551.
39 S. Rahdar, K. Pal, L. Mohammadi, A. Rahdar, Y. Goharniya, S. Samani and G. Z. Kyzas, *J. Mol. Struct.*, 2021, **1231**, 129686.
40 I. A. Kumar, A. Jeyaseelan, N. Viswanathan, M. Naushad and A. J. Valente, *J. Solid State Chem.*, 2021, **302**, 122446.
41 M. Saifuddin, J. Bae and K. S. Kim, *Water Res.*, 2019, **158**, 246–256.

Open Access Article. Published on 30 Thang Mi 2023. Downloaded on 01/06/2026 7:15:53 CH.
This article is licensed under a Creative Commons Attribution-NonCommercial 3.0 Unported Licence.

42 S. Rezania, A. Kadi, H. Kamyab, A. A. Ghfar, H. R. Nodeh and W. N. W. Ibrahim, *Chemosphere*, 2022, **307**, 135809.
43 G. B. Sisay, T. B. Atisme, Y. A. Workie, Z. W. Negie and M. L. Mekonnen, *Environ. Nanotechnol., Monit. Manage.*, 2023, **19**, 100766.
44 D. Ai, Y. Tang, R. Yang, Y. Meng, T. Wei and B. Wang, *Bioresour. Technol.*, 2023, 128598.
45 Z. Jia, W. Zeng, H. Xu, S. Li and Y. Peng, *Process Saf. Environ. Prot.*, 2020, **140**, 221–232.
46 T. Miyazato, N. Nuryono, M. Kobune, B. Rusdiarso, R. Otomo and Y. Kamiya, *J. Water Process. Eng.*, 2020, **36**, 101302.
47 H. Sereshti, E. Zamiri Afsharian, M. Esmaeili Bidhendi, H. Rashidi Nodeh, M. Afzal Kamboh and M. Yilmaz, *Environ. Prog. Sustainable Energy*, 2020, **39**, e13332.
48 P. Karthikeyan and S. Meenakshi, *J. Mol. Liq.*, 2019, **296**, 111766.
49 G. Italiya, M. H. Ahmed and S. Subramanian, *Environ. Nanotechnol., Monit. Manage.*, 2022, **17**, 100649.
50 F. M. Nasief, M. Shaban, K. A. Alamry, M. R. A. Khadra, A. A. P. Khan, A. M. Asiri and H. Abd El-Salam, *J. Environ. Chem. Eng.*, 2021, **9**, 105834.
51 Y. Cao, X. Wu, B. Li, X. Tang, X. Lin, P. Li, H. Chen, F. Huang, C. Wei and J. Wei, *Chemosphere*, 2023, **325**, 138378.
52 Y. Tao, B. Yang, F. Wang, Y. Yan, X. Hong, H. Xu, M. Xia and F. Wang, *Sep. Purif. Technol.*, 2022, **300**, 121825.
53 R. Nazarian, R. J. Desch and S. W. Thiel, *Colloids Surf., A*, 2021, **624**, 126813.
54 W. Xiong, J. Tong, Z. Yang, G. Zeng, Y. Zhou, D. Wang, P. Song, R. Xu, C. Zhang and M. Cheng, *J. Colloid Interface Sci.*, 2017, **493**, 17–23.
55 H. Liu, W. Guo, Z. Liu, X. Li and R. Wang, *RSC Adv.*, 2016, **6**, 105282–105287.
56 N. Cheng, B. Wang, Q. Feng, X. Zhang and M. Chen, *Bioresour. Technol.*, 2021, **340**, 125696.
57 Q. Yin, R. Wang and Z. Zhao, *J. Cleaner Prod.*, 2018, **176**, 230–240.
58 T. Wang, D. Zhang, K. Fang, W. Zhu, Q. Peng and Z. Xie, *J. Environ. Chem. Eng.*, 2021, **9**, 105184.
59 M. K. Nodeh, G. N. Bidhendi, M. A. Gabris, B. Akbari-adergani, H. R. Nodeh, A. Masoudi and S. Shahabuddin, *J. Braz. Chem. Soc.*, 2020, **31**, 116–125.
60 J. Huang, J. Zhou and M. Liu, *JACS Au*, 2022, **2**, 280–291.
61 A. Khan, S. Malik, N. Ali, M. Khurshid, M. Zubair, X. Gao, L. Ni and M. Bilal, in *Emerging Techniques for Treatment of Toxic Metals from Wastewater*, Elsevier, 2023, pp. 427–457.
62 N. Sohrabi, R. Mohammadi, H. R. Ghassemzadeh and S. S. S. Heris, *Microchem. J.*, 2022, **175**, 107087.
63 A. S. Eltaweil, A. M. Omer, H. G. El-Aqapa, N. M. Gaber, N. F. Attia, G. M. El-Subruiti, M. S. Mohy-Eldin and E. M. Abd El-Monaem, *Carbohydr. Polym.*, 2021, **274**, 118671.
64 T. Ahamad, M. Naushad and S. M. Alshehri, *J. Water Process. Eng.*, 2020, **36**, 101284.
65 I. Aswin Kumar, M. Naushad and N. Viswanathan, *J. Chem. Eng. Data*, 2020, **65**, 2712–2724.
66 S. Kumari, S. H. K. Annamareddy, S. Abanti and P. K. Rath, *Int. J. Biol. Macromol.*, 2017, **104**, 1697–1705.
67 A. El-Araby, L. El Ghadraoui and F. Errachidi, *Molecules*, 2022, **27**, 8285.
68 S. Liu, F. Fan, Z. Ni, J. Liu and S. Wang, *J. Cleaner Prod.*, 2023, **385**, 135649.
69 E. Zong, X. Wang, L. Zhang, J. Yang and X. Liu, *Molecules*, 2023, **28**, 2923.
70 Z. Chen, H. Luo and H. Rong, *Int. J. Biol. Macromol.*, 2020, **164**, 1183–1193.
71 M. Esmaeili Bidhendi, Z. Asadi, A. Bozorgian, A. Shahhoseini, M. A. Gabris, S. Shahabuddin, R. Khanam and R. Saidur, *Environ. Prog. Sustainable Energy*, 2020, **39**, 13306.
72 S. R. Yashas, B. Shahmoradi, K. Wantala and H. P. Shivaraju, *Polymer*, 2021, **233**, 124184.
73 Q. Hu, H. Liu, Z. Zhang and Y. Xie, *J. Mol. Liq.*, 2020, **309**, 113057.
74 I. A. Kumar, M. Naushad, T. Ahamad and N. Viswanathan, *Int. J. Biol. Macromol.*, 2021, **170**, 13–23.
75 S. Zhang, J. Ding and D. Tian, *J. Solid State Chem.*, 2022, **306**, 122709.
76 M. Keshvardoostchokami, S. Babaei, F. Piri and A. Zamani, *Int. J. Biol. Macromol.*, 2017, **101**, 922–930.
77 F. Yazdi, M. Anbia and S. Salehi, *Int. J. Biol. Macromol.*, 2019, **130**, 545–555.
78 M. L. Masheane, L. N. Nthunya, S. P. Malinga, E. N. Nxumalo and S. D. Mhlanga, *Phys. Chem. Earth*, 2017, **100**, 212–224.
79 E. Baigorria and L. F. Fraceto, *J. Cleaner Prod.*, 2022, **331**, 129867.
80 N. I. Ribeiro, O. B. Pessanha, M. L. G. S. Pessanha and D. Guimarães, *Sep. Purif. Technol.*, 2023, **307**, 122717.
81 E. Zong, G. Huang, X. Liu, W. Lei, S. Jiang, Z. Ma, J. Wang and P. Song, *J. Mater. Chem. A*, 2018, **6**, 9971–9983.
82 G.-J. Jiao, J. Ma, Y. Li, D. Jin, Y. Guo, J. Zhou and R. Sun, *Sci. Total Environ.*, 2021, **761**, 143217.
83 E. Zong, B. Guo, J. Yang, C. Shi, S. Jiang, Z. Ma and X. Liu, *ACS Omega*, 2020, **6**, 505–515.
84 T. Li, Z. Tong, Q. Zheng, H. Bao, A. Partow, S. Meng, L. Li and Y. C. Li, *ACS Sustain. Chem. Eng.*, 2021, **9**, 10468–10478.
85 A. Chinnathambi and T. A. Alahmadi, *Chemosphere*, 2021, **272**, 129851.
86 I. A. Kumar and N. Viswanathan, *Arabian J. Chem.*, 2020, **13**, 4111–4125.
87 A. Teimouri, S. G. Nasab, N. Vahdatpoor, S. Habibollahi, H. Salavati and A. N. Chermahini, *Int. J. Biol. Macromol.*, 2016, **93**, 254–266.
88 C. T. Vu and T. Wu, *J. Cleaner Prod.*, 2022, **379**, 134508.
89 T. Atnafu and S. Leta, *Heliyon*, 2021, **7**, e07973.
90 K. Zheng, L. Xiang, C. Huang, Y. Wang, H. Zhang and J. Li, *Colloids Surf., A*, 2022, **652**, 129719.
91 G. Nie, L. Wu, Y. Du, H. Wang, Y. Xu, Z. Ding and Z. Liu, *Chem. Eng. J.*, 2019, **360**, 1128–1136.
92 T. Jóźwiak, U. Filipkowska, P. Szymczyk, M. Kuczajowska-Zadrożna and A. Mielcarek, *Int. J. Biol. Macromol.*, 2017, **104**, 1280–1293.

© 2023 The Author(s). Published by the Royal Society of Chemistry

Open Access Article. Published on 30 Thang Mi 2023. Downloaded on 01/06/2026 7:15:53 CH.
This article is licensed under a Creative Commons Attribution-NonCommercial 3.0 Unported Licence.

93 H. Kong, J. Wang, G. Zhang, F. Shen, Q. Li and Z. Huang, *Sep. Purif. Technol.*, 2023, **320**, 124098.
94 B. Wang, X. Hu, D. Zhou, H. Zhang, R. Chen, W. Guo, H. Wang, W. Zhang, Z. Hong and W. Lyu, *J. Cleaner Prod.*, 2021, **298**, 126878.
95 S. Dong, Q. Ji, Y. Wang, H. Liu and J. Qu, *J. Environ. Sci.*, 2020, **89**, 102–112.
96 B. Liu, Y. Yu, Q. Han, S. Lou, L. Zhang and W. Zhang, *Int. J. Biol. Macromol.*, 2020, **157**, 247–258.
97 K. Y. Koh, Z. Chen, S. Zhang and J. P. Chen, *Chemosphere*, 2022, **286**, 131458.
98 X. Shan, L. Yang, Y. Zhao, H. Yang, Z. Xiao, Q. An and S. Zhai, *J. Colloid Interface Sci.*, 2022, **606**, 736–747.
99 V. Parimelazhagan, P. Yashwath, D. Arukkani Pushparajan and J. Carpenter, *Int. J. Mol. Sci.*, 2022, **23**, 12484.
100 N. N. Hau and D. Q. Huong, *J. Mol. Struct.*, 2023, **1277**, 134884.
101 A. Rajeswari, A. Amalraj and A. Pius, *J. Water Process. Eng.*, 2016, **9**, 123–134.
102 A. Ghamkhari, A. Rahdar, S. Rahdar and M. A. B. H. Susan, *Nano-Struct. Nano-Objects*, 2019, **19**, 100371.
103 P. Haseena, K. Padmavathy, P. R. Krishnan and G. Madhu, *Procedia Technol.*, 2016, **24**, 733–740.
104 J. Bian, A. Wang, Y. Sun and Q. Zhu, *Appl. Clay Sci.*, 2022, **225**, 106550.
105 F. Kassahun, A. M. Taddesse, E. Teju and Y. Bogale, *Groundw. Sustain. Dev.*, 2023, **20**, 100873.
106 W. Yang, X. Shi, J. Wang, W. Chen, L. Zhang, W. Zhang, X. Zhang and J. Lu, *ACS Appl. Mater. Interfaces*, 2019, **11**, 35277–35285.
107 P. Karthikeyan, H. A. T. Banu and S. Meenakshi, *Int. J. Biol. Macromol.*, 2019, **130**, 407–418.
108 Y. X. Huang, M. J. Liu, S. Chen, I. I. Jasmi, Y. Tang and S. Lin, *Water Environ. Res.*, 2019, **91**, 797–804.
109 L. Wang, T. Liang, Z. Chong and C. Zhang, *Environ. Sci. Pollut. Res.*, 2011, **18**, 38–45.
110 I. Kassem, E.-H. Ablouh, F.-Z. El Bouchtaoui, H. Hannache, H. Ghalfi, H. Sehaqui and M. El Achaby, *ACS Sustain. Chem. Eng.*, 2022, **10**, 15250–15262.
111 B. Pandey, P. Singh and V. Kumar, *Environ. Nanotechnol., Monit. Manage.*, 2021, **16**, 100596.
112 A. B. Sengul and E. Asmatulu, *Environ. Chem. Lett.*, 2020, **18**, 1659–1683.
113 Z. Yu, Q. Li, J. Wang, Y. Yu, Y. Wang, Q. Zhou and P. Li, *Nanoscale Res. Lett.*, 2020, **15**, 1–14.
114 I. Karkossa, A. Bannuscher, B. Hellack, W. Wohlleben, J. Laloy, M. S. Stan, A. Dinischiotu, M. Wiemann, A. Luch and A. Haase, *Sci. Total Environ.*, 2021, **801**, 149538.
115 S.-J. Chao, C. Huang, C.-C. Lam, L.-C. Hua, S.-H. Chang and C. Huang, *Ecotoxicol. Environ. Saf.*, 2021, **225**, 112759.
116 S. Sezer, A. Yücel, D. Ö. Turhan, F. B. Emre and M. Sarıkaya, *Chemosphere*, 2023, **325**, 138342.
117 M. Sun, R. Ding, Y. Ma, Q. Sun, X. Ren, Z. Sun and J. Duan, *Chemosphere*, 2021, **282**, 131124.
118 L. Ouyang, B. Chen, X. Liu, D. Wang, Y. Li, Y. Liao, K. W. Yeung and X. Liu, *Bioact. Mater.*, 2023, **21**, 520–530.
119 L. Li, T. Zhang, G. Zhang, G. Zhou, F. Yang, E. Wang, T. Liu and G. Wang, *Aquaculture*, 2022, **560**, 738579.
120 C. Liu, J. Ling, L.-Y. Yang, X.-k. Ouyang and N. Wang, *Carbohydr. Polym.*, 2023, **303**, 120436.
121 T. P. Rajesh, R. Balaji, S.-M. Chen, D. Nivetha, S. S. Rachel, N. Prakash, A. P. Steffi and C. Narendhar, *Inorg. Chem. Commun.*, 2021, **125**, 108447.
122 H. A. Sahyon, N. M. El-Shafai, N. Elnajjar, F. Althobaiti, A. Aldhahrani, N. S. Alharbi, A. G. F. Shoair and I. M. El-Mehasseb, *Int. J. Biol. Macromol.*, 2023, **234**, 123633.
123 Z. Wang, L. Song, N. Ye, Q. Yu, Y. Zhai, F. Zhang, M. G. Vijver and W. J. Peijnenburg, *NanoImpact*, 2020, **17**, 100211.
124 I. A. Kumar, C. Jeyaprabha, S. Meenakshi and N. Viswanathan, *Int. J. Biol. Macromol.*, 2019, **130**, 527–535.
125 H. A. T. Banu, P. Karthikeyan and S. Meenakshi, *Results in Surfaces and Interfaces*, 2021, **3**, 100010.
126 H. Luo, X. Zeng, P. Liao, H. Rong, T. C. Zhang, Z. J. Zhang and X. Meng, *Int. J. Biol. Macromol.*, 2019, **126**, 1133–1144.
127 T. Atnafu and S. Leta, *Heliyon*, 2021, **7**, e07973.
128 A. Ansari, E. T. Nadres, M. Đo and D. F. Rodrigues, *Process Saf. Environ. Prot.*, 2021, **150**, 365–372.
129 D. Jiang, X. Wang, L. Feng, Y. Yu, J. Hu, X. Liu and H. Wu, *Int. J. Biol. Macromol.*, 2022, **200**, 172–181.

© 2023 The Author(s). Published by the Royal Society of Chemistry